Impact parameter dependence of the electronic energy loss of low- and intermediate-energy protons in collisions with solid state atoms

1995 J. Phys.: Condens. Matter 7 3655

(http://iopscience.iop.org/0953-8984/7/18/027)

J. Phys.: Condens. Matter 7 (1995) 3655–3666. Printed in the UK

Impact parameter dependence of the electronic energy loss of low- and intermediate-energy protons in collisions with solid state atoms

Wang Neng-ping†, Ho Yu-kun†‡ and Pan Zheng-ying†§

† Department of Physics 2, Fudan University, Shanghai 200433, People's Republic of China
‡ CCAST (World Laboratory), PO Box 87730, Beijing, People's Republic of China
§ Ion Beam Laboratory, Shanghai Institute of Metallurgy, Academia Sinica, People's Republic of China

Received 24 August 1994, in final form 15 December 1994

Abstract. Using the linear-response dielectric theory and local electron density approximation, we calculate the electronic energy loss of low- and intermediate-energy protons in collision with a solid atom as a function of the impact parameter. In these studies, the correlation and exchange interaction of the electron gas in solids is taken into consideration by using a local field correction dielectric function. Based on the formalism electronic stopping cross-sections of protons in solids are calculated, and the results are compared with experimental data and empirical results, as well as with other previous theoretical results.

1. Introduction

The phenomenon of energy loss of high-energy protons has been studied thoroughly, and its general properties are reasonably well understood. But, the experiments yielding more detailed information on the stopping process have revived the interest in the problem. These studies include the study of the anomalously small energy loss under the channelling condition [1] and the angular dependence of energy loss [2–6]. The results of such experiments can only be interpreted if the dependence of energy loss on impact parameter in a proton collision with one of the medium atoms is known. The above-mentioned two types of experiment yield information on different impact parameter ranges. The stopping under the channelling condition is sensitive to the energy loss at high impact parameters ($p \geqslant a_0$; a_0 is the Bohr radius), whereas, the experiments studying the ejection angle dependence of energy loss yield information on the stopping process mainly at small impact parameters ($p \leqslant a_0$).

Theoretical studies of the impact parameter dependence of the energy loss are mainly made in terms of the semiclassical approximation which treats an incident proton as a classical particle moving along a definite, usually rectilinear, trajectory. The approaches used differ in the methods for describing the electron system and its excitation. Some works examined the stopping by an isolated atom whose excitation by the proton Coulomb field was described in terms of the first order of non-stationary perturbation theory [7–10]. A method based on a different principle for describing the electron excitation was used in [11–14] to calculate the impact parameter dependence of the energy loss. The stopping power of the electron gas was calculated in terms of the dielectric formalism. These works followed the Lindhard–Scharf concept [15] to calculate the energy loss in terms of the local

0953-8984/95/183655+12$19.50

electron density approximation (LDA) which treats each elementary atomic volume as a free electron gas whose density is a function of the distance from the centre of the atom.

Several theoretical investigations [16–18] have been made concerning calculations of the electronic stopping power. It has been found that the theoretical predictions for the electronic stopping power are in good agreement with experimental data in the high-velocity region; however, at lower velocities the agreement becomes poorer, especially below the maximum of the electronic stopping power curve. The discrepancies between the theories and experiments in this region are mainly due to the fact that the random phase approximation (RPA) dielectric function was used in all of those theoretical investigations. A slow proton can interact with many electrons of the electron gas along its path, so the correlation and exchange interaction of electrons at short range will be important. It is well known that because of the neglect of the correction and exchange interaction of the electron gas, the RPA dielectric theory is valid only in the weak-coupling limit of the interparticle correlations, i.e., $r_s < 1$ (where r_s is related to the density n_0 of the electron gas by $1/n_0 = 4\pi(r_s a_0)^3/3$, a_0 is the Bohr radius). In the electron gas of a metal, however, the values of r_s range from 1.5 to 5.88, so the RPA theory may not provide an accurate value of the stopping power. For a strongly coupled degenerate electron gas, going beyond the RPA description, Utsumi and Ichimaru [19] took into account the exchange and Coulomb correlational effects, and proposed a local field correlation (LFC) dielectric function.

In the present paper, we intend to combine the progress in these fields by making use of the LFC dielectric formalism and the LDA to calculate the impact parameter dependence of the electronic energy loss, and the stopping cross-section of low- and intermediate-energy protons in solids. The theoretical model is described in section 2. In section 3, we study the impact parameter dependence of the electronic energy loss of protons in solids. The stopping cross-section of protons in solids is investigated in section 4. Finally, we summarize our conclusions in section 5.

2. Theoretical model

2.1. Dielectric formalism

In Lindhard's linear-response theory the stopping power $(-\mathrm{d}E/\mathrm{d}x)$ of a proton moving in spatial homogeneous electron gas is given by

$$-\frac{\mathrm{d}E}{\mathrm{d}x} = \frac{2e^2}{\pi v^2}\int_0^\infty \frac{\mathrm{d}k}{k}\int_0^{kv} \mathrm{d}\omega\,\omega\,\mathrm{Im}\left[-\frac{1}{\epsilon(k,\omega)}\right] \tag{1}$$

where v is the proton velocity, and $\epsilon(k,\omega)$ is the longitudinal dielectric function for the electron gas. The dielectric function of the RPA theory can be expressed as

$$\epsilon(k,\omega) = 1 - P(k,\omega). \tag{2}$$

The polarizability $P(k,\omega)$ was given in [15].

When the Coulomb correlation and the exchange interaction of electrons at short distance are taken into consideration, the dielectric function is expressed by Utsumi and Ichimaru [19] as

$$\epsilon(k,\omega) = 1 - P(k,\omega)/[1 + G(k)P(k,\omega)] \tag{3}$$

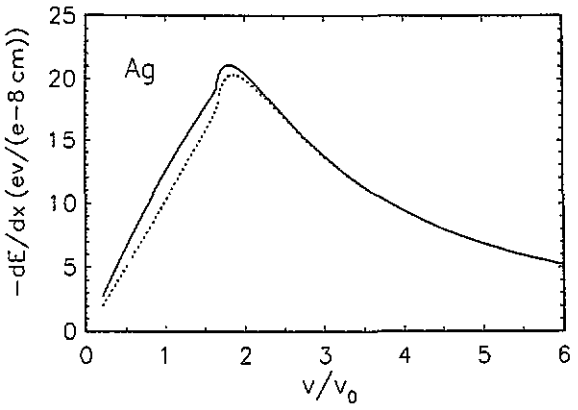

Figure 1. A comparison between the stopping powers $(-dE/dx)$ of a proton in the electron gas (with the density $n_0 = 6.601 \times 10^{-2}a_0^{-3}$, $r_s = 1.53$) of silver obtained from the LFC (the solid line) and the RPA (the short-dashed line) dielectric functions, respectively.

where $G(k)$ is the local field correction function. Introducing the dimensionless variables $z = k/2k_F$, where k_F is the Fermi wavenumber $k_F = (3\pi^2 n_0)^{1/3}$, $G(k)$ can be expressed as

$$G(z) = 16Az^4 + 4Bz^2 + C + (1/2z)(1-z^2)[16Az^4 + 4(B+8A/3)z^2 - C]\ln|(1+z)/(1-z)|. \tag{4}$$

In (4), $A = 0.029$, B and C are the functions of r_s

$$B = 9\gamma_0/16 - 3[1 - g(0)]/64 - 16A/15 \tag{5}$$

and

$$C = -3\gamma_0/4 + 9[1 - g(0)]/16 - 16A/5 \tag{6}$$

where $g(0) = \frac{1}{8}[z'/I_1(z')]^2$, $I_1(z')$ is a first-order modified Bessel function, $z' = 4(\alpha r_s/\pi)^{1/2}$, $\alpha = (4/9\pi)^{1/3}$, and the parameter γ_0 is connected to the correlation energy $E_c(r_s)$ by

$$\gamma_0 = 1/4 - (\alpha\pi r_s^5/24)\,\mathrm{d}[r_s^{-2}\,\mathrm{d}E_c(r_s)/\mathrm{d}r_s]/\mathrm{d}r_s \tag{7}$$

and

$$r_s\,\mathrm{d}E_c(r_s)/\mathrm{d}r_s = b_0(1 + b_1 r_s^{1/2})/(1 + b_1 r_s^{1/2} + b_2 r_s + b_3 r_s^{3/2}) \tag{8}$$

where $b_0 = 0.0621814$, $b_1 = 9.81379$, $b_2 = 2.82224$, and $b_3 = 0.736411$. Using equations (3)–(8), one can obtain the local field correction dielectric function. By use of equations (1) and (3)–(8), one can evaluate the electronic stopping power of protons in the strongly coupled degenerate electron gas.

In order to show the difference between the RPA and LFC dielectric theories, the electronic stopping powers $(-dE/dx)$ of a proton in the electron gas (with the density $n_0 = 6.601 \times 10^{-2}a_0^{-3}$, $r_s = 1.53$) of silver are calculated by using these two dielectric theories, and the results are shown in figure 1. From figure 1, it is found that in the low-energy range ($v \leqslant 2v_0$ for silver, v_0 is the Bohr velocity) the difference of the stopping powers $(-dE/dx)$ resulting from the RPA and LFC theories is obvious, but in the high-energy range these two theoretical results coincide with each other. We attribute this difference to the fact that a slow proton can interact with many electrons in the electron gas along its path, so the exchange and correlation interaction of the electron gas plays an important role in this case. In the high-energy range, the effect of the exchange and correlation interaction can be neglected.

For low velocities $v \ll v_F$, by making long-wavelength and low-frequency limit approximation in the LFC dielectric function, we can obtain the following expression:

$$-\frac{dE}{dx} = 4e^2 k_F^2 \chi^2 / 3(v/v_F) C(r_s) \tag{9}$$

where $C(r_s)$ was given in [20]. In figure 2, we show the result for the stopping power of a proton in the electron gas (with the density $n_0 = 6.601 \times 10^{-2} a_0^{-3}$, $r_s = 1.53$) of silver obtained from (9), and the corresponding result obtained from equations (1) and (3)–(8). From figure 2, one can find that the deviation is apparent when $v \geqslant 0.5v_0$, when $v = v_0$ the deviation is about 14%, and when $v = v_F \approx 1.25v_0$ the deviation is about 19%. This indicates that the short-wavelength effect in the dielectric function should be taken into consideration. In previous theoretical calculations, for instance in [13, 20], the low-frequency and long-wavelength limit approximation in the dielectric function was usually made in the velocity range $v \leqslant v_F$. From the above discussion, it is clear that the previous treatment is not stringent and causes a definite deviation.

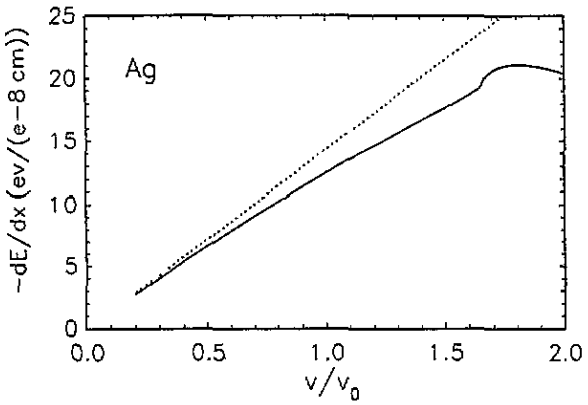

Figure 2. A comparison between the stopping powers $(-dE/dx)$ of a proton in the electron gas (with the density $n_0 = 6.601 \times 10^{-2} a_0^{-3}$, $r_s = 1.53$) of silver obtained from the low-frequency and long-wavelength limit approximation in the LFC dielectric function (short-dashed line), and by use of the LFC dielectric function determined by (3)–(8) (solid line).

2.2. *Local density approximation*

In principle, the electron wave functions and so the electron density in a solid can be obtained to within sufficient accuracy from the wave functions of a free atom in terms of the formalism of linear combination of atomic orbitals (LCAO). The LCAO calculations have shown that the valence shell electrons appear to be delocalized. The density of such electrons is nearly constant throughout most of the solid volume, so the valence shell electrons may be regarded as a uniform electron gas. We use the model of Gertner *et al* [16, 21], where the electron density of an atom in a solid is assumed to be constant n_0 in the outer region $(r > R)$ and slightly reduced in the inner region $(r < R)$ compared with the electron density $n_A(r)$ of the free atom. The electronic density has the following form:

$$n(r) = \begin{cases} n_A(r) + c_i & \text{if } r \leqslant R \\ n_0 & \text{if } R \leqslant r \leqslant R_0 \end{cases} \tag{10}$$

where c_i is a constant density correction, R_0 is the radius of an atom in a solid, which is determined from $\frac{4}{3}\pi R_0^3 = 1/\mathcal{N}$, $\mathcal{N}$ is the number of target atoms per unit volume, and R denotes the boundary radius between the outer region and the inner region of an atom in a solid. The constants n_0, c_i, and R are fixed by the following coupled equations:

$$\tfrac{4}{3}\pi(R_0^3 - R^3)n_0 = N_{\text{eff}} \tag{11}$$

$$4\pi \int_0^R r^2 n_A(r)\,dr + \frac{4}{3}\pi R^3 c_i = z_2 - N_{\text{eff}} \tag{12}$$

$$n_0 = c_i + n_A(R) \tag{13}$$

where N_{eff} is the effective number of electrons participating in the volume plasmon excitation as derived from the measured free electron plasma frequency and z_2 is the atomic number for the target.

The free atom electron density is determined from the analytic independent particle model for atoms after Green *et al* [22]. In this model the radial electron density is

$$4\pi r^2 n_A(r) = \frac{N}{d}\xi \frac{He^{\xi}}{(HT+1)^2}\left(-1 + \frac{2He^{\xi}}{HT+1}\right) \tag{14}$$

where $T = e^{\xi} - 1$, and $\xi = r/d$. N is the number of bound electrons in a given atom. The parameter H is determined as $H = 1.05dN^{0.4}$; d is an adjustable parameter.

We consider a local description of the energy loss. In terms of the electron density $n(r)$, the energy loss of the proton can be expressed as

$$-\frac{dE}{dx}(r) = \frac{4\pi e^4}{mv^2} n(r) L(n(r), v) \tag{15}$$

where $L(n(r), v)$ is the stopping number, and takes the form

$$L(n(r), v) = \frac{2}{\pi\omega_p^2}\int_0^{\infty}\frac{dk}{k}\int_0^{kv} d\omega\,\omega\,\text{Im}\left[-\frac{1}{\epsilon(k,\omega)}\right]. \tag{16}$$

In (16), $\omega_p^2 = 4\pi n(r)e^2/m$; ω_p is the plasma frequency.

Hence, we can write the energy transferred to the electrons $\Delta E(p, v)$, in a collision with the impact parameter p, as the line integral

$$\Delta E(p, v) = \int dl \left|\left[-\frac{dE}{dx}(r)\right]\right|_{r=r(l)} \tag{17}$$

where the integration is taken along the proton trajectory $r = r(l)$. When use is made of the straight-line approximation, the electronic energy loss of a proton in the collision with a solid atom can be written [12] as

$$\Delta E(p, v) = 2\int_p^{R_0} dr \frac{r}{\sqrt{r^2 - p^2}}\left(-\frac{dE}{dx}(r)\right). \tag{18}$$

The electronic stopping cross-section of protons in solids can be expressed as

$$S = 2\pi\int_0^{p_{\max}} \Delta E(p, v)p\,dp = 2\pi\int_0^{R_0} \Delta E(p, v)p\,dp. \tag{19}$$

3. Impact parameter-dependent electronic energy loss

By using the LFC dielectric formalism and the LDA, we calculated the electronic energy loss of protons in solids. In figure 3, we show the results of the electronic energy loss $\Delta E(p, v)$ of a proton scattering on an Al atom as a function of the impact parameter p, for various energies from 1 keV to 500 keV. From figure 3, one can find that the electronic energy loss $\Delta E(p, v)$ of a proton in a collision with a target atom decreases with increasing impact parameter. Furthermore, when the incident energy increases, the energy loss $\Delta E(p, v)$ decreases more strongly with the impact parameter. In figure 4, we show the obtained result for the energy loss of the proton with the energy $E = 100$ keV in a collision with an Al atom, compared with the experimental result [23] and another theoretical result [10]. From figure 4, it can be seen that the energy loss derived by us is in agreement with the main trend of the relevant experimental data. Our theoretical result is closer to the experimental result than the previous theoretical result [10], especially in the small-impact-parameter range ($p \leqslant a_0$). Figure 5 shows the calculated result for the energy loss of the proton with the energy $E = 200$ keV in collision with an Au atom, and the corresponding experimental results [24, 25] and previous theoretical result [10]. In figure 5, the energy loss of the proton in the range of large impact parameters ($p \geqslant a_0$) calculated by us is in agreement with the previous theoretical result [10], but deviates from the experimental results [24, 25]. As a whole, the agreement between the theoretical and experimental data is not very good. It should be noted, however, that the $\Delta E(p)$ dependence is very difficult to infer unambiguously from experimental data because of the allowance for multiple scattering in the target (see the discussion in [3–5, 12]). Besides, the effects arising from the impact parameter dependence of the energy loss may be veiled by inhomogeneities of the target thickness [26].

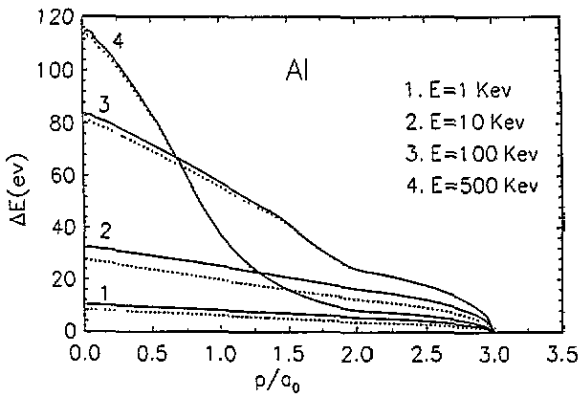

Figure 3. Electronic energy losses $\Delta E(p)$ versus impact parameter p for protons with incident energies from 1 keV to 500 keV scattering by Al, obtained from the LFC (solid lines) and the RPA (short-dashed lines) dielectric functions, respectively.

Figures 3–5 also give the theoretical results for $\Delta E(p)$ based on the RPA dielectric formalism and the LDA. From figure 3, we can see that in the range of low incident energies, the effect of the correlation and exchange interaction of the electron gas acts to enhance the values of electronic energy losses $\Delta E(p)$, while for high energies, the effect cannot be considered. In figures 4 and 5, there is very little difference between $\Delta E(p)$ obtained

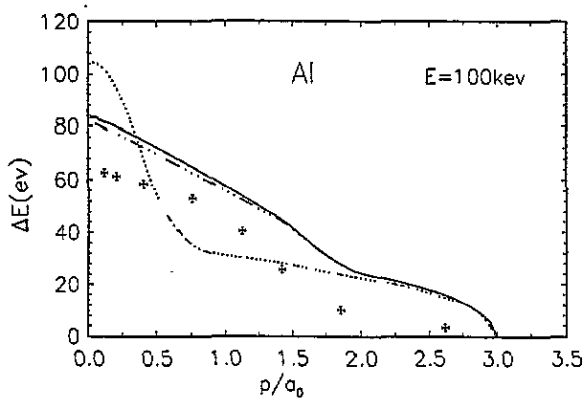

Figure 4. Electronic energy loss against impact parameter for protons with energy 100 keV scattering by Al. The solid line and the triple dot–dashed line are calculated by use of the LFC and the RPA dielectric functions, respectively. Dotted line: theoretical calculation result quoted from [10]. The crosses represent the experimental results [23].

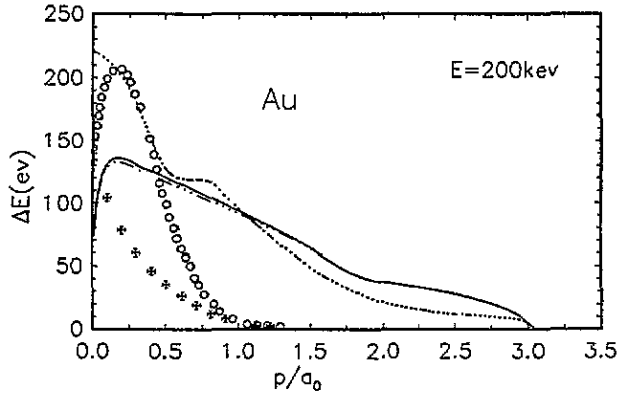

Figure 5. The same as in figure 4 for Au, and the proton energy of 200 keV. The crosses and circles show the experimental results from [24] and [25], respectively.

by use of the LFC and the RPA dielectric functions, in other words, for these energies, the correlation and exchange interaction is very weak.

4. Electronic stopping cross-section

By use of the LFC dielectric formalism and the LDA, the electronic stopping cross-sections of protons in solids, such as Ag, Au, Al, Ni, and Cu, have been evaluated, and the results are exhibited in figures 6–10. The associated parameters are listed in table 1. Ziegler *et al* [18] have proposed the empirical result for the electronic stopping cross-section of the hydrogen ion in all elements by the fit to all available experimental data. Recently, Paul *et al* [27] also proposed a new fit of the electronic stopping cross-section for hydrogen ion from about 10 to 2500 keV/nucleon for a few target elements, based on all the data in the literature (up to 1991). Because of the deviation for the experimental results of electronic

stopping cross-sections of protons in the low- and intermediate-energy range measured by different laboratories, and, also, in order to investigate the dependence of the stopping cross-section on incident energies within a wide region of incident energies, we choose the empirical results given by Ziegler *et al* and Paul *et al* as the reference stopping. From figures 6–10, it is clear that for high energies, our theoretical results are in good agreement with the empirical results, while for low energies, our results are very close to Paul *et al*'s empirical results. In addition, near the maximum of the electronic stopping curve, our results are slightly higher than the empirical results. However, we note that near the maximum of electronic stopping, the experimental data measured by different laboratories differ greatly and result in great uncertainty. To illustrate this uncertainty, we show two sets of experimental data near the maximum of electronic stopping in the figures. From those comparisons, one can find that our results are still within the range of experimental data.

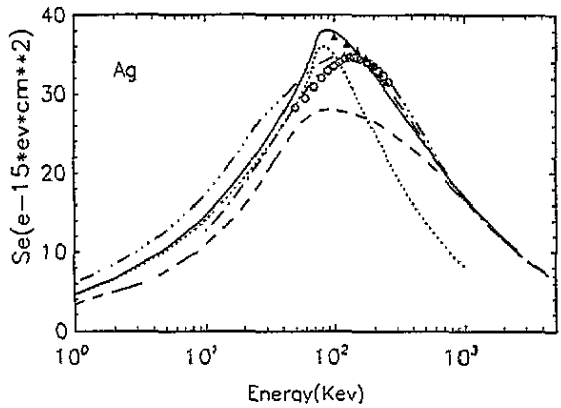

Figure 6. Electronic stopping cross-section of the proton in Ag as a function of the incident proton energy. The solid line is our calculation results based on the LFC dielectric formalism and the LDA. The triple dot–dashed and dash–dotted lines are empirical results given by Ziegler *et al* [18] and Paul *et al* [27] respectively. The long-dashed line is theoretical calculation results based on Lindhard stopping and the local density approximation quoted from [18]. The short-dashed line corresponds to our calculation results for the proton in the uniform valence electron gas (with the density n_0 given in table 1) using the LFC dielectric formalism. The circles and triangles are experimental data quoted from [28] and [29], respectively.

Table 1. Parameters used in the calculation.

	z_2	d^a	$\mathcal{N}a_0^3$	$n_0a_0^3$
Ag	47	0.754	8.685×10^{-3}	6.601×10^{-2}
Au	79	0.657	8.744×10^{-3}	7.246×10^{-2}
Al	13	0.729	8.928×10^{-3}	2.505×10^{-2}
Ni	28	0.700	1.354×10^{-2}	5.828×10^{-2}
Cu	29	0.606	1.258×10^{-2}	3.908×10^{-2}

[a] Quoted from [22].

In figure 6, we also show the Lindhard's theory result [18] based on the RPA dielectric formalism and the LDA. It can be seen that for high energies, our theoretical result based on the LFC dielectric formalism and LDA coincides with the Lindhard's theory result, while for

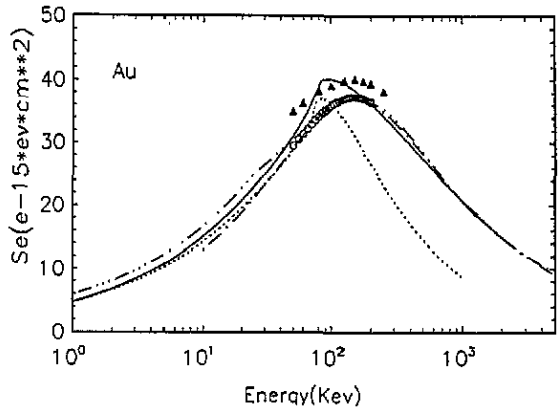

Figure 7. Electronic stopping cross-section for a proton on Au. The lines are defined as in figure 6. The circles and triangles are experimental data quoted from [30] and [31], respectively.

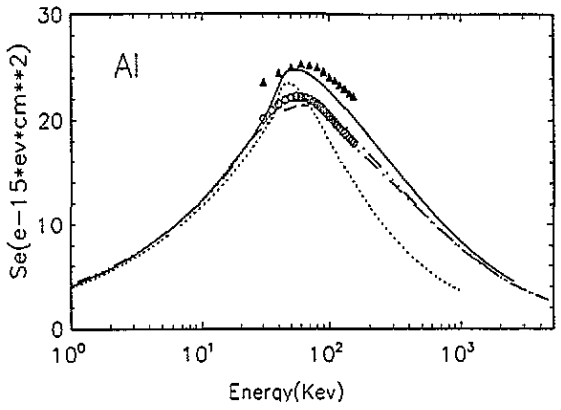

Figure 8. Electronic stopping cross-section for a proton on Al. The lines are defined as in figure 6. The circles and triangles are experimental data quoted from [30] and [28], respectively.

low and intermediate energies, our result is much closer to the empirical results than that of Lindhard's theory. This indicates that, for slow protons moving in metals, the exchange and correlation interaction of electrons at short range is important and should be taken into consideration.

In figures 6–10, we also show our theoretical result for the stopping cross-section of the proton in the uniform valence electron gas (with the density n_0 given in table 1) of metals using the LFC dielectric formalism. One can find that those are very close to the results based on the LFC dielectric formalism and the LDA in the low-energy range, and after the maximum of the electronic stopping the former decreases more strongly with increasing incident energy than the latter. This indicates that in the low-energy range, the proton mainly interacts with the valence electron gas in the outer region of a target atom, while in the high-energy range, the contribution to the electronic stopping from the inner-shell electrons becomes important and should be appropriately taken into consideration.

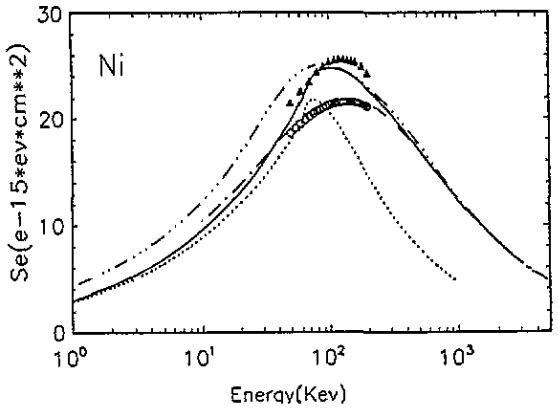

Figure 9. Electronic stopping cross-section for a proton on Ni. The lines are defined as in figure 6. The circles and triangles are experimental data quoted from [30] and [28], respectively.

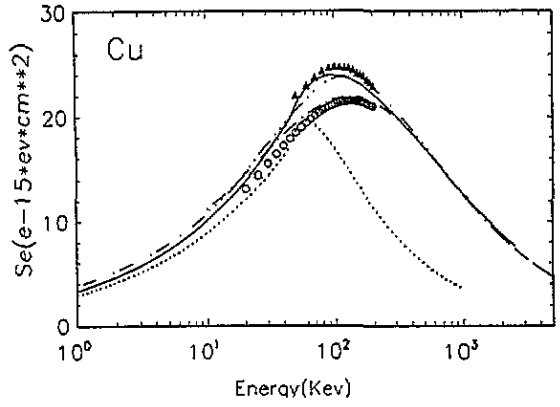

Figure 10. Electronic stopping cross-section for a proton on Cu. The lines are defined as in figure 6. The circles and triangles are experimental data quoted from [30] and [32], respectively.

5. Discussion and conclusion

Our study of the impact parameter dependence of the energy loss is based on several approximations. First we introduce the local field correction dielectric function created by Utsumi and Ichimaru [19] which takes into consideration the effects of correlation and exchange interaction of electrons at short range. Second, we introduce a local density approximation which permits us to integrate the energy loss, for a given impact parameter, along the trajectory of the proton. In addition, we make use of Gertner's model [16, 21] for the electron density of solid atoms, and Green's model [22] for the electron density of free atoms. In the velocity region $v \leqslant v_F$, we have found out that the short-wavelength effect in the dielectric function should be also taken into account.

In the small-impact-parameter range, our results for energy loss $\Delta E(p)$ are close to the experimental results. In the large-impact-parameter range, our result is very close to the previous theoretical result [10]. As a whole, the agreement between our results for the impact parameter dependence of proton energy losses and the experimental data inferred

from the angular dependence of energy loss is not very good. As pointed out by [10], the detailed comparison between theoretical and experimental data necessitates a more accurate allowance for the multiple-scattering effects and for the target thickness inhomogeneities.

By integrating $\Delta E(p)$ over impact parameters we make contact with the electronic stopping cross-section. This permits another check of the theoretical model. Our results for electronic stopping cross-section, based on the LFC dielectric formalism and the LDA, are in good agreement with the empirical results [18, 27]. A comparison of our theoretical results with those based on the RPA dielectric formalism and the LDA [18] is also made. In the low-energy region, our results are much closer to the empirical results than those in [18]. This indicates that in the low-energy range, the effect of the exchange and correlation interaction should be taken into consideration. By analysing the role of the LDA in the calculations, it is found that in the low-energy range, the electronic stopping mainly results from the valence electron gas in the outer region of the target atom, while in the high-energy range, the contribution to the electronic stopping from the inner-shell electrons is important and should be appropriately taken into consideration.

Acknowledgments

This work was supported by the China Postdoctoral Science Foundation and the Natural Science Foundations of China.

References

[1] Kumakhov M A and Komarov F F 1981 *Energy Loss and Ion Ranges in Solids* (London: Gordon and Breach)
[2] Iferov G A and Zhukova Yu N 1982 *Phys. Status Solidi* b **110** 653
[3] Bednyakov A A, Iferov G A, Kadmenskii A G, Naumova N M and Zhukova Yu N 1986 *Phys. Status Solidi* b **140** 63
[4] Ishiwari R, Shiomi N, Sakamoto N and Ogawa H 1986 *Nucl. Instrum. Methods* B **13** 111
[5] Eckardt J C, Lantschner G H, Jakas M M and Ponce V H 1984 *Nucl. Instrum. Methods* B **2** 168
[6] Jakas M M, Lantschner G H, Eckardt J C and Ponce V H 1983 *Phys. Status Solidi* b **117** K131
[7] Kitagawa M and Ohtsuki Y H 1972 *Phys. Rev.* B **5** 3418
[8] Dettmann K and Robinson M T 1974 *Phys. Rev.* B **10** 1
[9] Khodyrev V A and Sirotinin E I 1983 *Phys. Status Solidi* b **116** 659
[10] Kabachnik N M, Kondratev V N and Chumanova O V 1988 *Phys. Status Solidi* b **145** 103
[11] Winterbon K B 1983 *Radiat. Eff.* **79** 251
[12] Gras-Marti A 1985 *Nucl. Instrum. Methods* B **9** 1
[13] Ascolani H and Arista N R 1986 *Phys. Rev.* A **33** 2352
[14] Nagy I and Laszlo J 1985 *Phys. Lett.* **112A** 95
[15] Lindhard J and Sharff M 1953 *K. Danske Vidensk. Selsk. Mat.-Fys. Meddr.* **27** No 15
Lindhard J 1954 *K. Danske Vidensk. Selsk. Mat.-Fys. Meddr.* **28** No 8
[16] Gertner I, Meron M and Rosner B 1978 *Phys. Rev.* A **18** 2022
[17] Maynard G and Deutsch C 1982 *Phys. Rev.* A **26** 665
[18] Ziegler J F, Biersack J P and Littmark U 1985 *The Stopping Power and Ranges of Ions in Matter* (New York: Pergamon)
[19] Utsumi K and Ichimaru S 1982 *Phys. Rev.* A **26** 603
[20] Wang Y N and Ma T C 1990 *Nucl. Instrum. Methods* B **51** 216
[21] Gertner I, Meron M and Rosner B 1980 *Phys. Rev.* A **21** 1191
[22] Green A E S, Sellin D L and Zachor A S 1969 *Phys. Rev.* **184** 1
[23] Quoted from [10], and obtained by analysing the experimental data [5].
[24] Quoted from [10]. The result of the analysis of the experimental data [2, 3].
[25] Quoted from [10]. The result of the analysis of the experimental data [3, 6].
[26] Mertens P and Krist Th 1986 *Nucl. Instrum. Methods* B **13** 95

[27] Paul H, Semrad D and Seilinger A 1991 *Nucl. Instrum. Methods* B **61** 261
[28] Mertens P and Krist Th 1982 *Nucl. Instrum. Methods* **194** 57
[29] Santry D C and Werner R D 1981 *Nucl. Instrum. Methods* **188** 211
[30] Semrad D, Mertens P and Bauer P 1986 *Nucl. Instrum. Methods* B **15** 86
[31] Valenzuela A, Meckbach W, Kestelman A J and Eckardt J C 1972 *Phys. Rev.* B **6** 95
[32] Khodyrev V A, Mizgulin V N, Sirotinin E I and Tulinov A F 1984 *Radiat. Eff.* **83** 21